Bull. Mater. Sci., Vol. 10, Nos 1 & 2, March 1988, pp. 117–132. © Printed in India.

Role of stacking faults in solid state transformations

DHANANJAI PANDEY
School of Materials Science and Technology, Banaras Hindu University, Varanasi 221 005, India

Abstract. This article illustrates the two different roles played by stacking faults in solid state transformations viz. (i) in accommodating part of the transformation strains as observed in the noble metal-based alloys undergoing martensitic transformations, and (ii) in providing a mechanism for changing the stacking sequence of layers in a variety of materials like SiC, ZnS, Co and its alloys, and certain steels. Diffraction patterns taken from the martensitic phases of noble-metal-based alloys as well as from SiC and ZnS crystals undergoing transformation from one close-packed modification to another reveal the presence of characteristic diffuse streaks. It is shown that from a theoretical analysis of the observed intensity distribution along streaked reciprocal lattice rows in terms of physically plausible models for the geometry and distribution of faults, one can make a choice between various possible routes for transformation. From simple computer simulation studies, it is shown that the observed arrest of transformations in SiC is essentially due to the insertion of stacking faults in a random space and time sequence leading to an irregular distribution of solitons.

Keywords. Stacking fault; solid state transformation; martensitic transformation; noble metal-based alloys; computer simulation.

1. Introduction

Stacking faults are known to play two different roles during solid state structural transformations in two distinct class of materials. The noble-metal-based alloys, where martensitic transformation from the high temperature β/β_1 phase with a disordered/ordered bcc structure to β'/β_1' phase with close-packed structure has been extensively studied, belong to one such class of materials. The usual phenomenological crystallographic theories of martensitic transformation in these materials are based on the observation that the habit plane i.e. the matrix-martensite interface, remains undistorted in the average sense during the transformation. The transformation strains introduced by the 'lattice deformation shear' have therefore to be partly relieved by another kind of shear which should leave the lattice invariant but restore the undistorted character to the habit plane (Nishiyama 1978). The mode of 'lattice invariant shear' in the noble-metal-based alloys is experimentally found to be twinning or faulting on the close-packed planes. With the observation of shape memory effect in such internally faulted martensites, a phenomenon which was hitherto believed to be restricted only to internally twinned martensites, there has been an increased interest in the understanding of the nature of stacking faults involved in these transformations. In contrast to the noble-metal-based alloys where stacking faults provide a mechanism for strain accommodation, in materials like SiC, ZnS, Co and its alloys and certain steels, whose structure can be described by stacking of layers of atoms in the close-packed manner, stacking faults are known to bring about transformation from one stacking sequence of layers to another.

Diffraction patterns taken from noble-metal-based martensites frequently display the presence of characteristic diffuse streaks along c^*-direction revealing the presence

of stacking faults in these martensites. In the case of materials like SiC and ZnS, structural transformations are known to commence with the appearance of characteristic diffuse streaks joining the main reflections of the parent phase. As the transformation proceeds further, new reflections, which are considerably broadened and shifted from the regular Bragg positions, start appearing on the streaks indicating the development of a new stacking order in a statistical sense. From a theoretical analysis of the observed intensity distribution along streaked reciprocal lattice rows in terms of physically plausible models for the statistical insertion of stacking faults, it is possible to determine the crystallographic nature, distribution (random vs non-random) and the average concentration of stacking faults. Since the crystallographic nature and the type of distribution of faults are generally characteristic of the mechanism of transformation involved, it is possible to make a choice between various routes of transformation by making use of such a diffraction approach. This approach was originally developed in relation to the 2H to 6H transformation in SiC (Pandey *et al* 1980) and has since been applied to a variety of transformations in metallic and non-metallic systems (Pandey and Lele 1986a; Pandey *et al* 1986; Kabra *et al* 1986, 1988). One of the main purpose of the present article is to illustrate the application of the diffraction approach in elucidating the role of stacking faults in the two categories of transformations mentioned earlier.

In all the diffuse scattering studies due to stacking faults, the model employed for the analytical calculation of the intensity distribution along the diffuse streak is based on the assumption that the faults are inserted sequentially in a stack of layers from one end of the stack as in a typical random walk problem. Such a sequential model is realistic when the faults are introduced during the layer-by-layer growth of a crystal (Wilson 1942). However, faults responsible for solid state transformations are introduced in a pre-existing stack of layers in a random space and time sequence. In materials like SiC where the transformation mechanism prohibits the occurrence of faults below a certain minimum separation, there would be an upper limit, imposed by the offset between any two adjacently transformed regions, on the number of faults which can be inserted in the crystal in a random space and time sequence. The domain walls or the solitons formed by the impingement of the adjacently transformed regions may lead to an arrest of the transformation, a situation not predicted by the sequential model. In order to determine the upper limit to the number of faults and also to study the kinetics of these transformations, we have performed detailed computer simulation study of various transformations observed in SiC and ZnS. It is found that although the sequential model is not realistic for studying the evolution of these transformations, the theoretically predicted observable diffraction effects are not at variance with those obtained by simulation studies. We shall briefly describe the results of such a study in relation to the 2H to 6H transformation in SiC. Finally, it is suggested that the transformations observed in SiC and ZnS should be mapped into model one-dimensional competing interaction 3 state Potts/Ising systems to get a better insight into their kinetics.

2. Martensitic transformation in noble-metal-based alloys

In the copper-, silver- and gold-based alloys with a 3:2 electron-to-atom ratio, the β phase, which is bcc, is stable over a wide range of concentrations at high temperatures. At lower temperatures, the stability of the β-phase decreases leading to a

narrowing of the range of solid solution. In many of these alloys the β-phase finally undergoes a eutectoid decomposition into the equilibrium phases. However, rapid cooling suppresses the diffusion of atoms for the eutectoid reaction to take place and leads to a martensitic transformation. The structure of martensites can be described in terms of stacking of layers of atoms in the close-packed manner but the final symmetry depends on factors such as relative atomic radii of the constituent atoms and the formation of superlattices (Delaey *et al* 1982). The superlattices of the close-packed martensites are believed to result from the ordered parent phases which are distinguished from the disordered β phases by labelling them as β_1 or β_2 depending on whether the parent phase possessed DO_3 (Fe_3Al) or B2 (CsCl) type superlattice, respectively. The martensitic phases resulting from β, β_1 and β_2 phases are labelled as β', β'_1 and β'_2 respectively (Nishiyama 1978). In ternary systems such as Cu-Zn-Al, the parent phase may possess Heusler-type superlattice as well (Kajiwara 1976). Figure 1 depicts the phase diagram for the Cu-Al system. Table 1 gives the martensite phases formed in this system upon quenching. Here the primed layers are shifted with respect to the unprimed layers through $b/2$ along the [010] direction of the ortho-hexagonal unit-cell (Nishiyama 1978). This shift is inherited from the DO_3

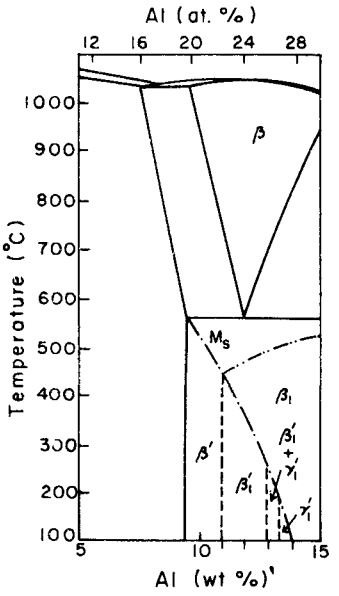

Figure 1. Phase diagram for Cu-Al system (after Nishiyama 1978).

Table 1. Martensite phases formed in the Cu-Al system.

Composition range (wt.%)	Martensite produced	Ramsdell and Zhdanov notations	Symmetry	Layer stacking sequence
<11%	β'	$9R\,(12)_3$	Trigonal	$A_+B_-A_-C_+A_-C_-B_+C_-B_-$
11–13%	β'_1	$18R\,(12)_6$	Orthorhombic	$A_+B'_-A_-C'_+A_-C'_-B_+C'_-$ $B_-A'_+B_-A'_-C_+A'_-C_-B'_+C_-B'_-$
> 13%	γ'_1	2H (11)	Orthorhombic	$A_+B'_-$

superlattice of the β_1-phase and causes the doubling of the number of layers in the [001] direction. In this section we shall concentrate on the two different mechanisms for bcc (β) to 9R (β') transformation and the role of stacking faults in accommodating the transformation strains. From the experimentally observed orientation relationships between the parent and the product phases, it has been confirmed that the basal plane (001) of the martensite originates from the $\{110\}$ planes of the parent.

In the phenomenological crystallographic theories of the formation of β'/β'_1 martensites from the β/β_1 parent phase, the transformation is visualized to occur by the operation of a lattice deformation shear followed by a lattice invariant shear (Nishiyama 1978). While the original WLR theory of martensitic transformation was aimed at providing a rationale for the crystallographic observables such as the orientation relationships, the habit plane and the transformation shape strain, Nishiyama and Kajiwara (1963), and Chakravorty and Wayman (1977) have proposed a mechanism for the β/β_1 to the β'/β'_1 transformation in the same framework. According to Nishiyama and Kajiwara (1963), the first step in the lattice deformation shear is the formation of the $(001)_{\beta'/\beta'_1}$ close-packed basal plane from a, say, $(101)_{\beta/\beta_1}$ plane through expansions along $[10\bar{1}]_{\beta/\beta_1}$ and $[101]_{\beta/\beta_1}$ and a contraction along $[010]_{\beta/\beta_1}$. This step is followed by a homogeneous shear in the $[1\bar{1}0]$ direction of the β/β_1 phase giving rise to a close-packed structure with ABC, . . stacking. Homogeneous shear in directions other than $\pm[1\bar{1}0]$ is not permitted on the basis of geometrical considerations. For the perfect β' (9R) or β'_1 (18R) martensite to result, a reverse shear, called shuffling, has to occur on every third $(110)_{\beta/\beta_1}$ planes. This, according to Chakravorty and Wayman (1977), should require passage of Shockley partials on every third layer of the intermediate fcc phase. All the aforesaid steps including shufflings constitute the so-called 'lattice deformation shear' of the phenomenological theory. As a result, the habit plane, which is experimentally observed to be undistorted, gets distorted. To restore the undistorted character of the habit plane, inhomogeneous shear, which leaves the lattice invariant, is envisaged in the phenomenological theory. In the β' and β'_1 martensites, the mode of lattice invariant shear is experimentally observed to be faulting. According to Chakravorty and Wayman (1977), deformation faults bordered by $\frac{1}{3}$ [100] type Shockley partials are involved in the lattice invariant mode of shear. There are three possible deformation fault configurations in the 9R structure. In the notation described elsewhere (Pandey 1984), these faults can be written as

$I_{0,1}$: . . . A B A C A C B C B A_0 ⋮ C_1 B A B A C A C B . . .
$I_{1,2}$: . . . A B A C A C B C B A B_1 ⋮ C_2 B C B A B A C A . . .
$I_{2,0}$: . . . A B A C A C B C B A B A_2 ⋮ B_0 C B A B A C A C . . .

Here the dotted vertical line indicates the location of the shear plane. Of the three fault configurations, $I_{1,2}$ and $I_{2,0}$ are crystallographically equivalent and need not be distinguished from each other. The theoretically calculated lattice invariant shear involving deformation faults is in excellent agreement with the experimentally observed values (Kajiwara 1976). Thus, according to this mechanism, a preformed β'/β'_1 phase is inhomogeneously faulted through the passage of Shockley partials bordering deformation faults. Chakravorty and Wayman (1977) performed a detailed transmission electron microscopic investigation of β'_1 martensites and found no evidence for the periodically-spaced Shockley partials required for the shufflings but

they have claimed to have observed inhomogeneously distributed Shockley partials at the β_1/β'_1 interface which might be responsible for the lattice invariant shear. Figure 2 illustrates this mechanism schematically.

The alternative mechanism for the β/β_1 to β'/β'_1 transformation is due to Ahlers (1974) and has been neatly summarized by Andrade *et al* (1984). According to this model, a homogeneous shear on the $(011)_{\beta/\beta_1}$ planes in the $[0\bar{1}1]_{\beta/\beta_1}$ direction transforms the $(101)_{\beta/\beta_1}$ planes into close-packed layers as shown in figures 3a, b. After this homogeneous shear, atoms on these close-packed layers are not in a stable position with respect to those on planes just above and below as depicted in figure 3c by a position like D'. The stable positions, such as those indicated by D'' and D''', can be achieved by shufflings in the $D'D''$ or $D'D'''$ directions. If the shear occurs in the same direction for the successive close-packed layers of atoms, a face-centred cubic structure ($ABC, \ldots$) will result while the movement of two consecutive layers in the

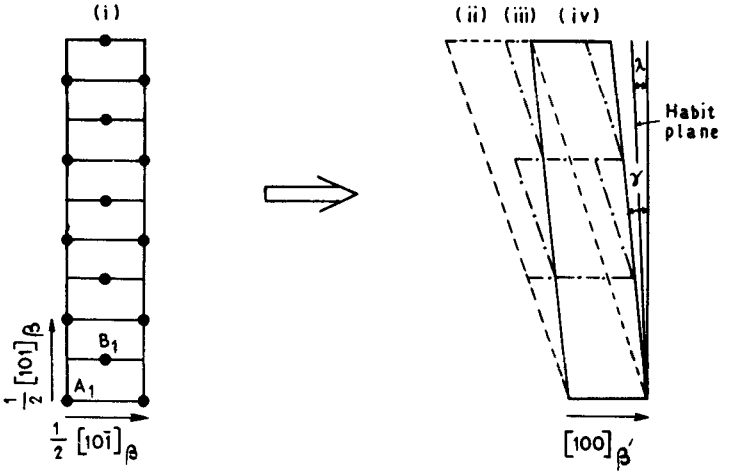

Figure 2. Lattice deformation and lattice invariant shears during β to β' martensitic transformation. (i) Stacking of $(101)_\beta$ phase layers prior to transformation, (ii) $ABC\ldots$ stacking is generated by expansions along $[10\bar{1}]_\beta$ and $[101]_\beta$ and a contraction along $[010]_\beta$ followed by a homogeneous shear on (001) $[\bar{1}00]_{\beta'}$, (iii) If the structure in (ii) is shuffled on (001) $[100]_{\beta'}$ on every third close-packed layer, the 9R(β') structure is formed. (iv) γ is the net shear required to produce the β' phase from β. In order to maintain the invariant habit plane, extra lattice invariant shear is required leaving a net shear of $\lambda(<\gamma)$ only (after Chakravorty and Wayman 1977).

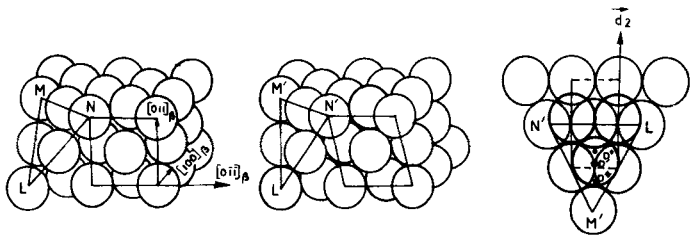

Figure 3. (**a**) Stacking of $(011)_\beta$ planes. (**b**) The first shear through $1/18\ [0\bar{1}1]_\beta$ transforms the plane LMN in (a) into the close-packed plane $LM'N'$. (**c**) Stacking positions of the LM'N' close-packed planes. The displacement during the second shear are in the d_2 direction on this plane (after Andrade *et al* 1984).

$D'D''$ direction followed by the third layer moving in the opposite $D'D'''$ direction will lead to a 9R/18R martensite. Since $2D'D''+D'D'''=0$, the contribution of shuffling to the lattice deformation shear is zero. However, due to the constraints imposed by the coexistence of the β/β_1 and β'/β'_1 phases, the habit plane will not remain invariant. In order that the exact invariant habit plane is created, it is essential that some of the close-packed planes formed after the first shear undergo wrong shuffles such as three successive layers, rather than just two moving in the $D'D''$ direction followed by a layer shuffling in the $D'D'''$ direction. Such wrong shuffles will give rise to stacking faults which have been termed as sequence faults by Andrade *et al* (1984). A single violation of the shuffling rule will lead to the following three types of sequence faults:

$$I_{0,0}: \ldots . A^{+}B^{-}A^{-}C^{+}A^{-}C^{-}B^{+}C^{-}B^{-}A_0^{-} \vdots \quad C_0^{+}A^{-}C^{-}B^{+}C^{-}B^{-}A^{+}B^{-}A \ldots$$

$$I_{1,1}: \ldots . A^{+}B^{-}A^{-}C^{+}A^{-}C^{-}B^{+}C^{-}B^{-}A^{+}B_1^{+} \vdots C_1^{-}B^{-}A^{+}B^{-}A^{-}C^{+}A^{-}C^{-}B \ldots$$

$$I_{2,1}: \ldots . A^{+}B^{-}A^{-}C^{+}A^{-}C^{-}B^{+}C^{-}B^{-}A^{+}B^{-}A_2^{+} \vdots B_1^{-}A^{-}C^{+}A^{-}C^{-}B^{+}C^{-}B^{-}A \ldots$$

The dotted vertical line indicates the position of the fault plane with respect to the 9R sequence on its left hand side. The symbols + and − correspond to shufflings in the $D'D'''$ and $D'D''$ directions, respectively, while the arrow marks the single violation of the shuffling rule. Note that after the violation, the direction of shuffling is adjusted to restore the normal + − − sequence.

Thus, in this picture, faults are formed not after the formation of a sizeable region of the β'/β'_1 phase but during the layer-by-layer shufflings of the close-packed layers, obtained after the homogeneous shear deformation, to maintain an undistorted habit plane in an average sense. This model conforms well to the definition of martensitic transformation proposed by Olson *et al* (1979). That the atomic movements during the β/β_1 to β'/β'_1 transformation are correctly described by the Ahlers model is supported by the following two observations: (i) softening of the elastic constants corresponding to $\langle 011\rangle\ \{0\bar{1}1\}$ shear system on approaching M_s and (ii) a lowering in the phonon dispersion curves of β phase at $q=\frac{2}{3}q_{\max}\{\xi\xi 0\}$ (Guenin and Gobin 1978; Guenin *et al* 1979).

There are essentially three energy terms involved in the β/β_1 to β'/β'_1 transformation: the change in the chemical-free energy (ΔG^{chem}), the strain energy and the stacking fault energy. In the first mechanism, the strain energy at the habit plane is relieved by the nucleation of Shockley partials bordering deformation faults in the already formed sizeable region of the β'/β'_1 martensite phase. In the second mechanism, the shuffling direction for each layer of the martensitic phase is decided by the minimization of the total energy comprising the three terms. If the total energy is lowered by wrong shuffles, stacking faults will be incorporated in the layer-stacking sequence. It is not possible to distinguish between the two mechanisms for the lattice invariant shear on the basis of the habit plane and the total transformation shear calculation since both will yield the same values for the following reasons. The three sequence faults can be visualized as the consequence of wrong shuffles through 1/3 [100] type vectors during an intermediate hypothetical fcc to β'/β'_1 transformation occurring at one-, two- and four-layer separations. Thus the lattice-invariant shear by both sequence as well as deformation faults can geometrically be visualized to involve the same partial slip vectors although mechanistically, the two processes are distinct.

For the 'normal' 9R and 18R modifications (for details of 'normal' and 'modified' β'/β'_1 martensites, reference is made to Delaey *et al* (1982) observed in the Cu-Al system, it has been shown by Andrade *et al* (1984) that the conventional transmission electron microscopic technique using $\bar{g}.\bar{R}$ criterion cannot be employed to distinguish between 'sequence' and 'deformation' type faults since both are simultaneously visible or invisible for all the permissible reflections of 9R/18R. Recently we have shown that a distinction between the sequence and deformation faults can be made even in the normal 9R and 18R martensites by analysing the intensity distributions along diffuse streaks (Kabra *et al* 1987). We have developed the relevant theory of diffraction for 9R crystals containing a random distribution of sequence and deformation faults. It is found that the theoretically predicted observable diffraction effects, such as sense of the shifts from the normal Bragg positions and the broadening of the otherwise sharp reflections, are markedly different for the sequence and deformation faults. Indeed it is also possible to distinguish amongst the various sequence faults themselves on the one hand and the various deformation faults on the other. Figures 4 to 6 depict the calculated intensity distribution for these faults with fault probabilities $\alpha=0{\cdot}1$, $\alpha=0{\cdot}3$ and $\alpha=0{\cdot}5$. It is evident from these figures that the peak shifts for the sequence faults are in the positive or negative directions for different reflections in one period of 9R. For deformation faults, all the reflections are shifted either in the positive or in the negative directions. The peak shifts reported in the literature by Nishiyama *et al* (1965) and Kajiwara (1976) for the faulted β' and β'_1 martensites are of mixed type

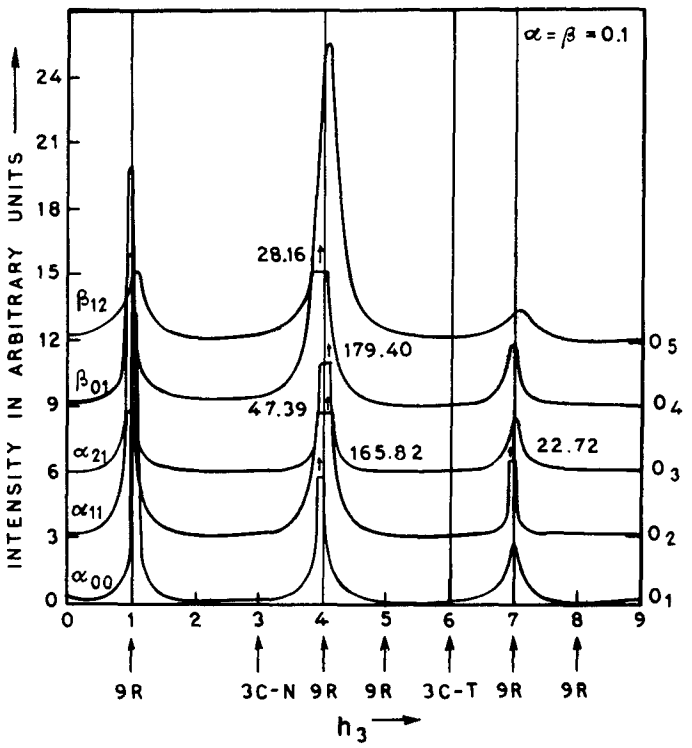

Figure 4. Intensity distribution along diffuse streak for a 9R crystal containing randomly distributed $I_{0,0}$, $I_{1,1}$, $I_{2,1}$, $I_{0,1}$ and $I_{1,2}$ faults: fault probability = 0·1.

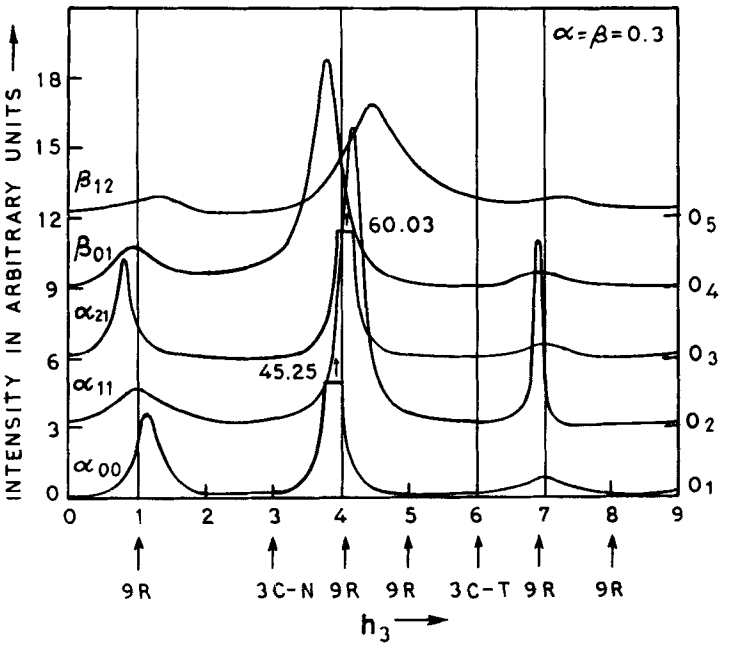

Figure 5. Intensity distribution along diffuse streak for a 9R crystal containing randomly distributed $I_{0,0}$, $I_{1,1}$, $I_{2,1}$, $I_{0,1}$ and $I_{1,2}$ faults: fault probability = 0·3.

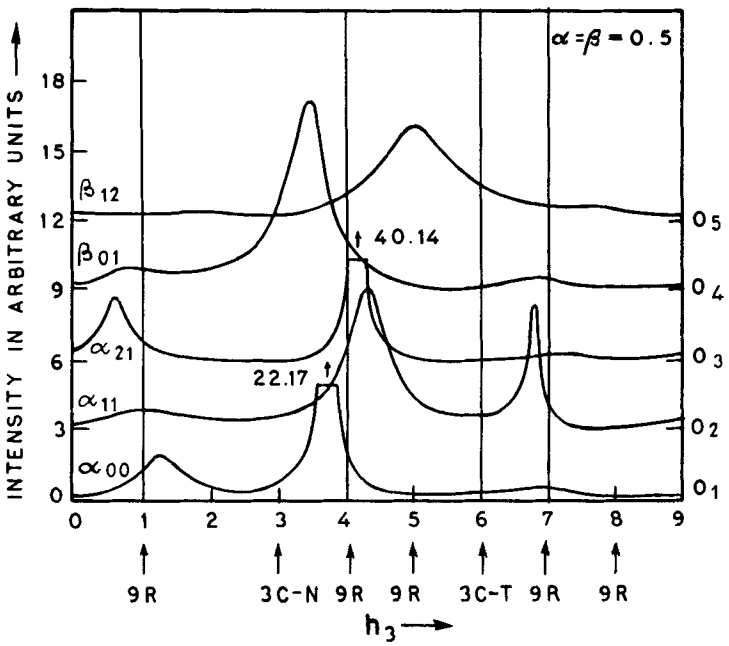

Figure 6. Intensity distribution along diffuse streak for a 9R crystal containing randomly distributed $I_{0,0}$, $I_{1,1}$, $I_{2,1}$, $I_{0,1}$ and $I_{1,2}$ faults: fault probability = 0·5.

i.e. both positive and negative, for various reflections in one period. This fact thus rules out the presence of deformation faults in these martensites. Our conclusion is also in agreement with the electron microscopic studies of Cook *et al* (1983) and Delaey *et al* (1984) for the modified β'/β_1' martensites.

3. Solid state transformations in SiC

α-Silicon carbide crystals are grown above 2000°C from the vapour phase and contain numerous polytypic modifications whose structure can be described in terms of different possible stacking sequence of Si-C double layers in the close-packed manner. 6H with a layer stacking *ABCACB*, . . . is the most common modification amongst these crystals. The long period polytypes are believed to result by accidents during spiral growth round screw dislocations created in a perfect or faulted basic matrices (for details see Pandey and Krishna 1982, 1983). The 3C (*ABC*, . . .) or β-SiC crystals usually grow at temperatures below 2000°C. The 2H (*AB*, . . .) modification has never been found to occur in α-SiC crystals and has been synthesized around 1400°C by special methods in the presence of impurities. Structural transformations in single crystals of 2H and 3C modifications of SiC have been investigated by several workers (Krishna *et al* 1971; Krishna and Marshall 1971a, b; Jagodzinski 1971; Tagai *et al* 1971; Powell and Will 1972). A common characteristic of these transformations is that they commence with a statistical insertion of stacking faults giving rise to characteristic diffuse streaks along certain reciprocal lattice rows. As the transformation proceeds further, intensity modulations along the diffuse streaks giving rise to the appearance of broad elongated spots, characteristic of the product phase, are observed. The final structure is invariably observed to be highly faulted indicating arrest of the transformation. It has been reported that the 2H structure transforms to a disordered-twinned 3C structure, when the transformation commences at temperatures between 1400°C and 1600°C. The resulting 3C structure on further annealing above 1600°C transforms to a disordered 6H structure. This indicates that the cubic structure may be stable upto 1600°C, beyond which the 6H modification is stable. 2H crystals in which transformation commences above 1600°C indeed transform to disordered 6H structure. The 3C crystals also transform to 6H on annealing above 1600°C.

We have performed a detailed theoretical and experimental study of the 2H to 6H and the 3C to 6H transformations in SiC to determine the nature of stacking faults responsible for these transformations. Since the geometrical nature of stacking faults is generally characteristic of the mechanism of transformation involved, we have been able to choose between two alternative mechanisms of transformations in SiC (Pandey *et al* 1980; Pandey *et al* 1986; Kabra *et al* 1986). In this section we shall briefly describe the results of our investigation for the 2H to 6H transformation.

The structural transformations in SiC can result either by a layer displacement mechanism or by a deformation mechanism. The 2H to 6H transformation by the layer displacement mechanism would require the layer displacement faults to occur preferentially on every third close-packed layers as depicted below.

Initial structure (2H): . . . A B **A** B A **B** A B **A** B A **B** . . .
Resulting structure (6H): . . . A B **C** B A **C** A B **C** B A **C** . . .

The layer displacement faults may get nucleated at high temperatures by the aggregation of vacancies in a small region of a close-packed layer in the *AB* . . . structure followed by the diffusion of atoms into *C* sites within this region. If the size of the nucleus is greater than a certain critical size, the region of the *C* layer will spread to cover the entire plane provided this leads to a lowering of the energy (Pandey and Krishna 1974). The same 2H to 6H structural transformation can also result by the deformation faults occurring preferentially after every three close-packed layers as depicted below:

Initial structure (2H): A B|A B A B A B A B A B . . . .
C A C|A C A C A C A . . . .
B A B|A B A B . . . .
C A C|A . . . .
B . . . .

Resulting structure (6H): A B C A C B, A B C A C B . . . .

The deformation faults necessary for the transformation may either be present already in the 2H crystal or may be nucleated by thermal stresses at high temperatures.

In both the mechanisms, the occurrence of the layer displacement or deformation faults would be a statistical phenomenon but there would be a tendency for the faults to occur in such a manner as to minimize the free energy and take the structure towards the stable state. If the stable state happens to be one with a different structure, such a structure will tend to result. Thus in both the cases, the transformation will commence with the statistical insertion of faults giving rise to continuous streaks joining the reciprocal lattice rows parallel to c^* with $H\text{-}K \neq 0$ mod 3. Pronounced intensity maxima will appear on these streaks at a later stage and eventually form the regular diffraction spots characteristic of the stable structure.

In order to make a choice between the layer displacement and deformation mechanisms, we have developed (Pandey *et al* 1980; Pandey *et al* 1986) the theory of X-ray diffraction from one-dimensionally disordered 2H crystals undergoing transformation to the 6H structure by each mechanism. It should be noted that the diffraction theory developed by Christian (1954) and Sato (1969), for a completely random distribution of deformation and layer displacement faults in the 2H structure, cannot be applied to 2H crystals undergoing transformation to the 6H structure, because in this case the faults are not distributed entirely at random but prefer to occur in such a manner as to statistically create a 6H structure. To take this into account in the theory, we have assumed that once the fault occurs on a particular layer, it cannot occur on the next two layers in the structure. Accordingly we define a fault probability α/β which is the probability of occurrence of a layer displacement/deformation fault such that the next two layers cannot be faulted. For $\alpha \cdot \beta = 0$, the structure is perfect 2H while for $\alpha/\beta = 1$, the structure is perfect 6H. Thus the faults can occur at a minimum separation of three layers. Using this model, we have performed a detailed mathematical calculation of the diffracted intensity and observable diffraction effects for different fault probabilities. Figures 7 and 8 depict the theoretically calculated intensity distribution along the 10. L reciprocal lattice row for the layer displacement and the deformation mechanisms respectively.

For a 2H crystal undergoing solid state transformation to the 6H structure by the layer displacement mechanism, the following diffraction characteristics may be predicted on the basis of figure 7: (i) the reflections $L = 0$ mod 2 and $L = \pm 1$ mod 2 of the 2H structure remain sharp and unbroadened (i.e. δ-peaks) throughout the transformation although their intensities change, (ii) in the beginning of the transformation diffuse elongated reflections develop at positions approximately midway of the 2H reflections with $L = 0$ mod 2 and $L = \pm 1$ mod 2, (iii) as the concentration of the layer displacement faults increases, each diffuse reflection splits into two distinct reflections and these gradually approach the positions of the normal 6H reflections at $L = \pm \frac{1}{3}$ mod 2 and $L = \pm \frac{2}{3}$ mod 2. For $\alpha < 1$, the diffuse 6H reflections are shifted towards each other.

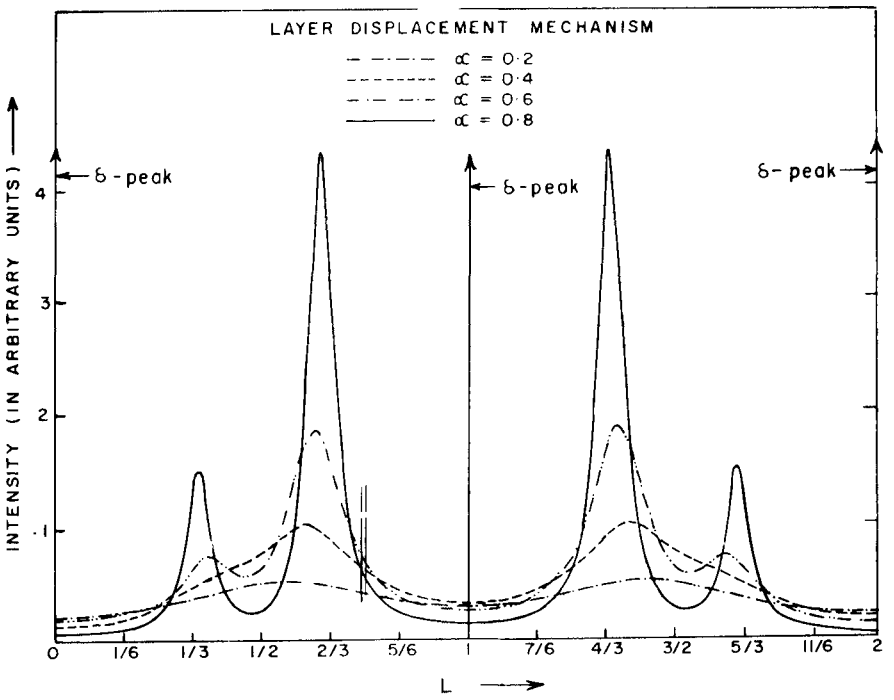

Figure 7. Calculated intensity distribution along diffuse streak for crystals undergoing 2H to 6H transformation by non-random insertion of layer displacement faults for fault probabilities $\alpha = 0{\cdot}2$, $0{\cdot}4$, $0{\cdot}6$ and $0{\cdot}8$.

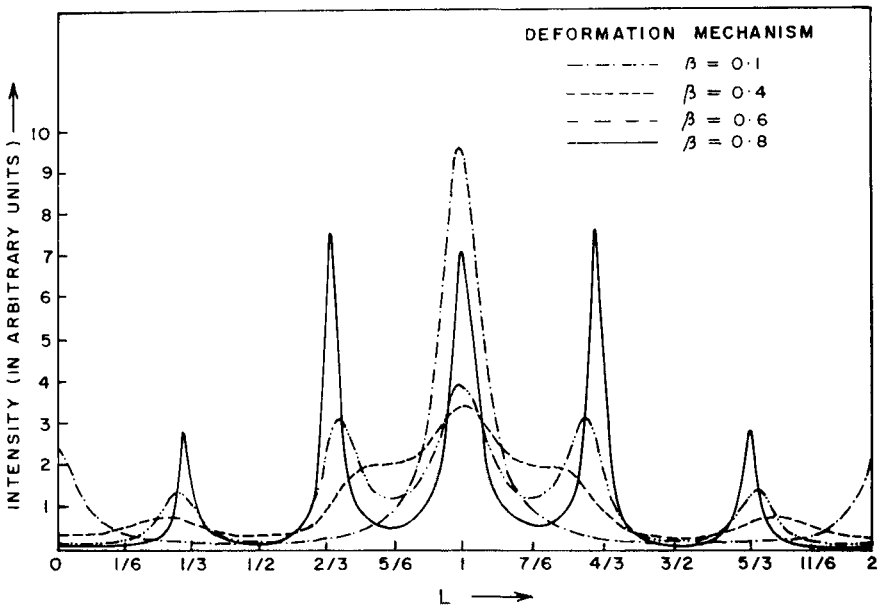

Figure 8. Calculated intensity distribution along diffuse streak for crystals undergoing 2H to 6H transformation by non-random insertion of deformation faults for fault probabilities $\beta = 0{\cdot}1$, $0{\cdot}4$, $0{\cdot}6$ and $0{\cdot}8$.

On the other hand the main diffraction characteristics of a crystal undergoing the 2H to 6H transformation by the deformation mechanism, as deduced from figure 8, are: (i) the transformation commences with the broadening of the 2H reflections, (ii) new reflections characteristic of the 6H structure initially appear near positions with $L = \pm \frac{1}{6}$ mod 2 and $L = \pm \frac{5}{6}$ mod 2 and gradually move away from these positions and finally approach the positions with $L = \pm \frac{1}{3}$ mod 2 and $L = \pm \frac{2}{3}$ mod 2. In this case the 6H reflection are shifted away from each other for $\beta < 1$.

From a comparison of the theoretically predicted diffraction effects with those experimentally observed on single crystal X-ray diffraction patterns, we have shown that the 2H to 6H transformation in SiC takes place by the layer displacement mechanism. Figure 9a gives the $10{\cdot}L$ reciprocal row of a 2H SiC crystal annealed above 1600°C for several hours. The diffuse elongated spots midway of the 10·0 and $10{\cdot}\pm1$ reflections of 2H developed after the heat treatment and can be understood in terms of the layer displacement mechanism only. Figure 9b gives the intensity distribution as measured on a 4-circle single crystal diffractometer along the $10{\cdot}L$ row of a 2H SiC crystal, partially transformed to 6H by annealing above 2000°C for 16 hours. It is evident from this figure that the 6H reflections are shifted towards each other, as predicted for the layer displacement mechanism. We have recently carried out a similar investigation of the 3C to 6H transformation in SiC and have shown that this transformation also takes place by the layer displacement mechanism (Kabra *et al* 1986). It should be noted that while a layer displacement fault in the 2H structure requires displacement of single layer, in the 3C structure, this requires transposition of a pair of layers. Layer displacement faults in both the 2H and the 3C structures are faults with zero displacement vector in the sense defined by Paidar (1985) and cannot therefore be characterized by the usual $\bar{g}.\bar{R}$ criterion of the conventional electron microscopy since $|\bar{R}|$ is now zero.

4. Computer simulation studies

It was shown in the previous section that a choice between the deformation and layer displacement mechanisms for the 2H to 6H transformation can be made from a study of the intensity distributions along diffuse streaks. In all such studies the method employed for the calculation of the diffracted intensities makes use of the sequential (or unidirectional) insertion of faults in a stack of layers from one end of the stack. The fault probability (α/β) is defined as the probability of occurrence of a fault such that the next two layers are not faulted, as one performs a random walk from one end of the stack towards the other. Thus the faulted layer along with the two succeeding unfaulted layers are the consequence of one step in the random walk. Consider a stack of N close-packed layers in the 2H crystal. Let n be the number of faulted layers introduced in this stack for the 2H to 6H transformation. Since after each faulted layer we add two layers without fault, the number of random steps available being (N-2n). Since the fault probability is the ratio of the number of faults to the number of random steps available, we have

$$\alpha = n/(N-2n) = (n/N)/(1-2n/N) = f/(1-2f),$$

or
$$f = \alpha/(1+2\alpha), \tag{1}$$

where f is the fraction of faulted layers.

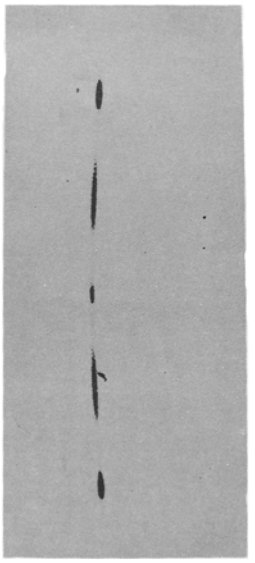

(a)

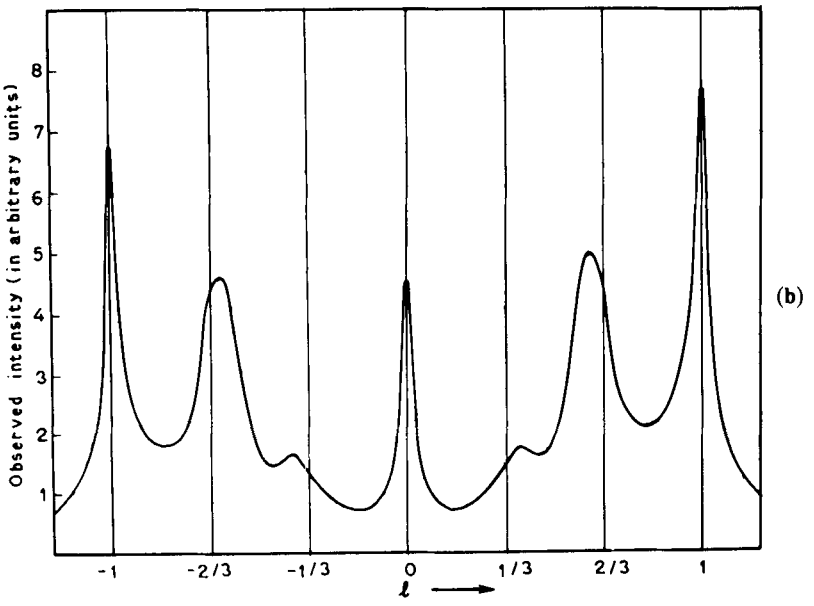

(b)

Figure 9. (**a**) The 10·*L* reciprocal lattice row, as recorded on an oscillation photograph, of a partially transformed 2H SiC crystal after annealing for several hours above 1600°C. The development of elongated diffuse spots midway of 2H reflections 10·0 and 10·±1 is notable (CuK radiation, Camera radius 3 cm, × 3). (**b**) Observed intensity distribution along the 10·*L* reciprocal lattice, as measured on a 4-circle diffractometer, of a 2H SiC crystal, after partial transformation to 6H. Vertical lines indicate the positions of X-ray reflections for the perfect 6H structure.

The sequential model for the insertion of faults is physically realistic when faults arise during the layer-by-layer growth of a crystal. However in crystals undergoing structural transformations through faulting, faults are introduced in a random space and time sequence rather than sequentially from one end of the crystal. Since the

transformation mechanism usually prohibits the occurrence of faults below a certain minimum separation (3 layers for the 2H to 6H case), there would be an upper limit on the number of faults which can be inserted in a random space and time sequence in the stack due to the off-set between adjacently transformed regions. Such an upper limit to the number of faults, and hence the sequential fault probability, dictated by the real situation is not implicit in our earlier calculations. Thus calculations for fault probabilities higher than this upper limit, although permissible in the sequential model, do not correspond to physical reality. One would also like to compare the intensity distributions obtained for the sequential and the random space model for the same value of the fraction of faulted layers. In order to achieve the twin objectives, we have recently studied the random spatial insertion of layer displacement faults in a stack of 1200 layers of 2H labelled from 1 to 1200. Layers for faulting were selected using integer random variables [1, 1200]. Each time a fault was inserted, say at the layer labelled n_1, the layers labelled n_1-2, n_1-1, n_1+1 and n_1+2 were precluded for the occurrence of faults. The process of random site selection, faulting and blocking of two layers on either side was performed until no more faults could be inserted. Figure 10 depicts the evolution of the 2H to 6H transformation in a small portion of the actual ensemble of 1200 layers, as the fraction of faulted layers increases from 0·083 to 0·187 to 0·277 after which no more faults could be introduced. Ideally, in the sequential model with one fault in every three layers, one expected a total of 400 faults in a stack of 1200 layers. Thus $f=0{\cdot}277$ against the expected value of 0·333 corresponds to the arrest of the transformation. We have also numerically computed the diffracted intensities corresponding to the three stages of evolution shown in figure 10 (Kabra and Pandey 1987). It is found that the observable diffraction effects, such as the non-broadening of 2H reflections and appearance of diffuse elongated spots midway of the 2H reflections predicted on the basis of the sequential model, are borne out by the simulation studies. This implies that corresponding to each simulated configuration, there exists a sequential analogue with a characteristic fault probability α which is related to the fraction of faulted layers in accordance with equation (1).

The off-set between the adjacently transformed 6H regions will lead to solitons. In a 6H structure, random impingement of 6H regions can in principle lead to 14 unique soliton configurations enumerated elsewhere by the author (Pandey 1984) but due to the restriction imposed on the minimum separation between two layer displacement faults only two of the fourteen possible soliton configurations are observed. These are marked as $I_{2,5}$ and $I_{2,1}$ in the notation described by Pandey (1984). The arrested configuration with $f=0{\cdot}277$ ($\alpha=0{\cdot}62$) thus corresponds to a 6H phase with a large number of irregularly distributed solitons of the two kinds. It is interesting to note that the two soliton configurations do not broaden the 6H reflections common with 2H (Kabra *et al* 1986) in perfect agreement with the prediction for the 2H to 6H transformation by a sequential insertion of layer displacement faults.

The fact that the end-product of the 2H to 6H transformation is experimentally found to be invariably a disordered 6H structure suggests that the irregularly distributed solitons are strongly pinned to the lattice and that they cannot be completely removed without melting. There is no evidence for these solitons to give rise to a higher order commensurate phase based on the 6H structure. This transformation thus provides an example of global chaos along the stacking axis of the close-

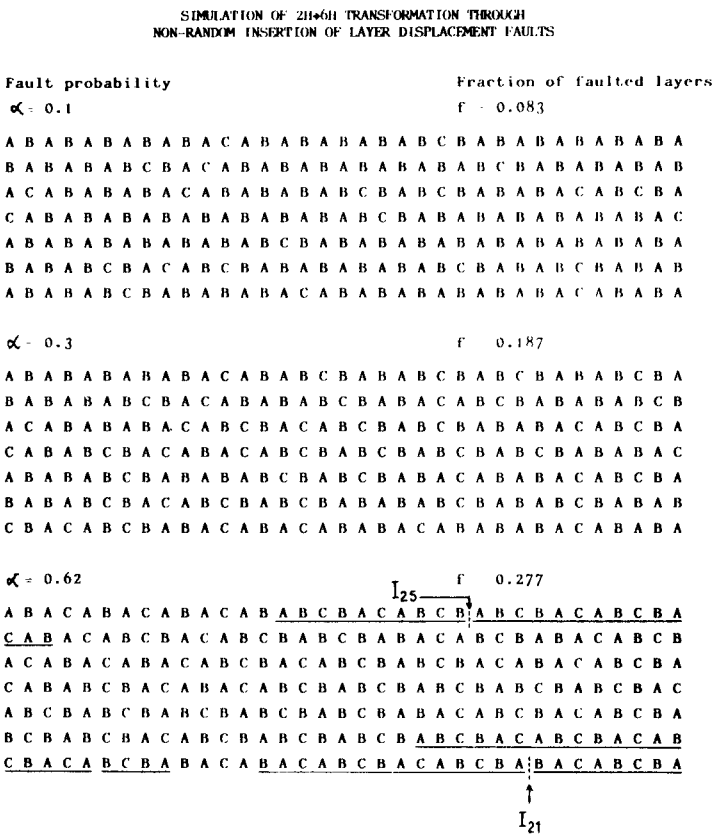

Figure 10. Computer simulation results of the evolution of 2H to 6H transformation by layer displacement mechanism with various fractions of faulted layers. The transformation gets arrested at $f = 0{\cdot}277$.

packed layers. A better insight into the kinetics of such transformations and the time scales involved in the transformation from chaotic to a regular 6H crystal can be provided by mapping the transformation mechanisms in terms of magnetic spin flips either for an Ising system or a three-state Potts system. One can then perform Monte Carlo spin flips using a suitable Hamiltonian incorporating competing interactions in a direction perpendicular to the close-packed layers. Such a study is presently underway and the preliminary results are very encouraging.

Acknowledgements

The author wishes to acknowledge collaborations with V K Kabra, S Lele and P Krishna for various pieces of work described above. Interesting discussions with T V Ramakrishnan, H R Krishnamurthy, S Shenoy, Deepak Kumar, M Barma and Deepak Dhar are gratefully acknowledged. Part of the work presented in this article was completed during the author's tenure as a Homi Bhabha Fellow for which he is grateful to the Council of Homi Bhabha Fellowships.

References

Ahlers M 1974 *Z. Metall.* **65** 636

Andrade M, Chandrasekaran M and Delaey L 1984 *Acta Metall.* **32** 1809

Chakravorty S and Wayman C M 1977 *Acta Metall.* **25** 989

Christian J W 1954 *Acta Crystallogr.* **7** 415

Cook J M, O' Keefe M A, Smith D J and Stobbs W M 1983 *J. Microscopy* **129** 295

Delaey L, Chandrasekaran M, Andrade M and Van Humbeeck J 1982 in *Proc. Int. Conf. on Solid Solid Phase Transformations* (eds) H I Aaronson, D E Laughlin, R F Sekerka and C M Wayman, (Warrendale: Met. Soc. of AIME) p 1429

Guenin G and Gobin P F 1978 *Scr. Metall.* **12** 351

Guenin G, Hautecler S, Pynn A, Gobin P F and Delaey L 1979 *Scripta Metall.* **13** 429

Jagodzinski H 1971 *Kristallogr.* **16** 1235

Kabra V K and Pandey D 1988 (to be published)

Kabra V K, Pandey D and Lele S 1986 *J. Mater. Sci.* **21** 1654

Kabra V K, Pandey D and Lele S 1988 *Acta Metall.* (In Press)

Kajiwara S 1976 *Trans. Jpn. Inst. Metals.* **67** 435

Krishna P and Marshall R C 1971a *J. Cryst Growth* **9** 319

Krishna P and Marshall R C 1971b *J. Cryst. Growth* **11** 147

Krishna P, Marshall R C and Ryan C E 1971 *J. Cryst. Growth* **11** 129

Nishiyama Z and Kajiwara S 1963 *Jpn. J. Appl. Phys.* **2** 478

Nishiyama Z, Kakinoki J and Kajiwara S 1965 *J. Phys. Soc. Jpn.* **20** 1192

Nishiyama Z 1978 *Martensitic transformation* (New York: Academic Press)

Olson G B, Cohen M and Clapp P C 1979 *Proc. of ICOMAT-79*, Cambridge, Mass., p.1

Paidar V 1985 *Philos. Mag.* **52** 73

Pandey D 1984 *Acta Crystallogr.* **B40** 567

Pandey D, Kabra V K and Lele S 1986 *Bull Mineral.* **109** 49

Pandey D and Krishna P 1973 in Proc. 3rd Intern. Conf. SiC, Florida, University of South Carolina Press, p. 198

Pandey D and Krishna P 1982 in *Current topics in materials science* (ed.) E Kaldis, (Amsterdam: North Holland) Vol. 9, p 415

Pandey D and Krishna P 1983 *Progr. Cryst. Growth Charact.* **7** 213

Pandey D and Lele S 1986 a, b *Acta Metall.* **34** 405, 415

Pandey D, Lele S and Krishna P 1980a b, c *Proc. R. Soc. (London)* **A369** 435, 451, 463

Powell J A and Will H A 1972 *J. Appl. Phys.* **43** 1400

Sato R 1969 *Acta Crystallogr.* **A25** 387

Tagai T, Sueno S and Sadanaga R 1971 *Miner. J.* **6** 240

Wilson A J C 1942 *Proc. R. Soc. (London)* **A180** 268